Proceedings Paper:
Bhowmik, D. and Abhayaratne, C. (2009) Embedding distortion modeling for non-orthonormal wavelet based watermarking schemes. In: Proc. SPIE 7248, Wavelet Applications in Industrial Processing VI. SPIE 7248, January 18, 2009, San Jose, CA. , 72480K-72480K. ISSN: 0277786X.

https://doi.org/10.1117/12.810719

Embedding Distortion Modeling for Non-orthonormal Wavelet Kernel based Watermarking Schemes

Deepayan Bhowmik and Charith Abhayaratne

Department of Electronic and Electrical Engineering, University of Sheffield, Sheffield, S1 3JD, United Kingdom.

ABSTRACT

In this paper a universal embedding distortion model for wavelet based watermarking is presented. The present work extends our previous work on modelling embedding distortion for watermarking algorithms that use orthonormal wavelet kernels to non-orthonormal wavelet kernels, such as biorthogonal and non-linear wavelets. By using a common framework for major wavelet based watermarking algorithms and the Parsevals energy conservation theorem for orthonormal transforms, we propose that the distortion performance, measured using the mean square error (MSE), is proportional to the sum of energy of wavelet coefficients to be modified by watermark embedding. The extension of the model to non-orthonormal wavelet kernel is obtained by rescaling the sum of energy of wavelet coefficients to be modified by watermark embedding using weighting parameters that follows the energy conservation theorems in wavelet frames. The proposed model is useful to find optimum input parameters, such as, the wavelet kernel, coefficient selections and subband choices, for a given wavelet based watermarking algorithm.

Keywords: Watermarking, wavelet, distortion performance, non-orthonormal wavelet kernel.

1. INTRODUCTION

Digital watermarking attracts major attention from the researchers and industries, as a latest protection tool for multimedia in digital right management. Often watermarking algorithms adopt a base technology based on the state of the art compression schemes. For example, a numerous number of wavelet based watermarking schemes[1–11] are proposed by the researchers due to the standardisation of wavelet based JPEG2000 compression scheme. Though many independent algorithms are available in the literature, a gap has been identified which requires a generalised mathematical analysis to identify the relationship between distortion performance and various input parameters, responsible for embedding distortion. Few works[12] have been carried out towards this problem but they mainly focused on their own algorithms.

In our previous work[13] we addressed this issue and came out with a generalised model for embedding distortion for wavelet based watermarking schemes. This model generalised all major wavelet based schemes under one common platform and presented a mathematical relationship between distortion performance metric such as mean square error (MSE) and responsible input parameters including wavelet kernels, subband selection and coefficient selection. The said model was constructed on orthonormal bases which conserves energy in the signal domain and the transform domain. Thus this model is only valid for orthonormal wavelet kernels such as Haar, Daubechies-4, or Daubechies-8.

To give a universal acceptance of the model we have extended our work which includes non-orthonormal wavelet bases such as biorthogonal and non-linear wavelet kernels. The rest of the paper is organised with a brief discussion of the previous work and the propositions made, in Sec. 2. The extended new analysis is presented in Sec. 3 followed by example simulation results in Sec. 4. Section 5 includes concluding remarks on this universal embedding distortion model.

Email: {d.bhowmik, c.abhayaratne}@sheffield.ac.uk (Send correspondence to Charith Abhayaratne).

2. DISTORTION PERFORMANCE MODEL FOR ORTHONORMAL WAVELET BASES

A generalised distortion performance model for wavelet based watermarking scheme is presented in.[13] The model is analysed and verified with orthonormal wavelet kernels. In the said model two different goals have been achieved: generalisation of wavelet based embedding schemes and the effect of input parameters on distortion performance. We shall discuss these briefly in order to provide sufficient background for the extension of this work for non-orthonormal wavelet bases.

2.1 The common framework for wavelet based watermark embedding

Although many different wavelet based watermarking schemes available, it possible to accommodate most of them in a common formal framework[14] by dissecting them into common functional blocks. In most of the algorithms the basic embedding principle remains same and the modified coefficient $C'_{m,n}$ at (m,n) position, can be presented as:

$$C'_{m,n} = C_{m,n} + \Delta_{m,n}, \tag{1}$$

where $C_{m,n}$ is the coefficient to be modified and $\Delta_{m,n}$ is the modification due to watermark embedding. The modification algorithms can broadly be divided in two groups: direct modification[1,2,7,10,11] and quantisation based modification.[3,4,6,8]

2.1.1 Direct modification

Direct modification algorithms are generalised in the following modification value $\Delta_{m,n}$ at (m,n) position:

$$\Delta_{m,n} = (a_1)\alpha(C_{m,n})^b W_{m,n} + (a_2)v_{m,n}W_{m,n} + (a_3)\beta C_w + (a_4)S_{m,n}, \tag{2}$$

where $a_1, ..., a_4$ are boolean variables to identify the presence of each of the components for a given methodology, $C_{m,n}$ is the coefficient to be modified, α is the watermark weighting factor, $b = 1, 2...$ is the watermark strength parameter, $W_{m,n}$ is the watermark value, $v_{m,n}$ is the weighting parameter based on pixel masking in HVS model, β is the weighting parameter in the case of fusion based scheme, C_w is the watermark wavelet coefficient and $S_{m,n}$ is any other value which is normally a function of $C_{m,n}$. In most of the algorithms watermark weighting parameters α and β are user defined to an optimal value.

2.1.2 Quantisation based modification

In this case, the modification ($\Delta_{m,n}$) is performed based on a ranked order quantisation update. The median value of a local area (typically a 3x1 coefficient window) is usually modified to a quantised step and the quantisation step δ ($-\delta \leq \Delta \leq \delta$) is decided upon a local minima (C_{min}) and local maxima (C_{max}) of the selected window coefficients. The expression to determine δ varies in different algorithms.

The realisation of different wavelet based watermarking algorithms using the common framework, are described in Tab. 1. As the watermark information or a weighting parameter is fixed and user defined often the modification value Δ is either a function of the selected coefficient $C_{m,n}$ or a local minima (C_{min}) and maxima (C_{max}).

2.2 Embedding Distortion Performance Analysis

In this mathematical model a relationship is established between distortion performance metric and the watermark embedding parameters. Based on the Parseval's energy conservation theorem a set of propositions have been made and proved in .[13] Here we have described the propositions which are based on the orthonormal wavelet bases and the extension of the same for the non-orthonormal bases are described in the next section.

Proposition 1. *Sum of the noise power in the transform domain is equal to sum of the noise power in the input signal for orthonormal transforms. If the input signal noise is defined by $\Delta x[n]$ and the noise in transform domain is $\Delta y[k]$ then*

$$\sum_n |\Delta x[n]|^2 = \sum_k |\Delta y[k]|^2, \tag{3}$$

Table 1. Realisation of wavelet based algorithms using different combination of input parameters

Method	Selection Coeff $< a_1, a_2, a_3, a_4 >$	Subband Selection	Wavelet Kernel	Level	Reference	Δ as Function of
Direct($b = 2$)	$< 1, 0, 0, 0 >$	High	Haar	2	[1]	$f(C_{m,n})$
Direct($b = 1$)	$< 1, 0, 0, 0 >$	All	Biorthogonal	3	[2]	$f(C_{m,n})$
Direct($b = 1$)	$< 1, 0, 0, 0 >$	Low	Biorthogonal, Non-linear	3	[15]	$f(C_{m,n})$
Direct	$< 0, 0, 1, 0 >$	High	Orthogonal	4	[11]	$f(C_{m,n})$
Direct	$< 0, 0, 0, 1 >$	High	Any	2	[10]	$f(C_{m,n})$
Quantisation	-	Low	Any	2	[6]	$f(C_{min}, C_{max})$
Quantisation	-	High	Haar	1	[4]	$f(C_{min}, C_{max})$
Quantisation	-	High	Any	2	[3]	$f(C_{min}, C_{max})$

where $n \in Z$ is the length of the input signal and $k \in Z$ is the length in the transform domain, respectively.

Proof. For the proof our previous work[13] is requested to refer.

Now using *Proposition 1* and the common generalised framework the relationships are stated between the modification energy sum in the coefficient domain to embed the watermark and the distortion performance metrics.

Proposition 2. *In a wavelet based watermarking scheme, the mean square error (MSE) of the watermarked image is directly proportional to the sum of the energy of the modification values of the selected wavelet coefficients. The modification value itself is a function of the wavelet coefficients and therefore we propose two different cases based on the categorisation.*

Case A. *For the direct modification embedding method the modification is a function of the selected coefficient to be watermarked and the relationship between MSE (P_p) and the selected coefficient ($C_{m,n}$) is expressed as:*

$$P_p \propto \sum |f(C_{m,n})|^2. \tag{4}$$

Case B. *For the quantisation based method the modification is a function of the neighbouring wavelet coefficients of the selected median coefficient to be watermarked and the relationship between MSE (P_p) and the wavelet coefficients C_{min} and C_{max} is expressed as:*

$$P_p \propto \sum |f(C_{min}, C_{max})|^2. \tag{5}$$

Proof. For the proof our previous work[13] is requested to refer.

3. EMBEDDING DISTORTION PERFORMANCE ANALYSIS FOR NON-ORTHONORMAL WAVELET BASES

In this section we have extended our previous propositions for non-orthonormal wavelet bases. We recall embedding distortion performance metric mean square error (MSE) which is defined as follows:

Definition 1. The *Mean Square Error (MSE)* or average noise power P_p in pixel domain between original image I and watermarked image I' is defined by:

$$P_p = \frac{1}{MN} \sum_{j=0}^{M-1} \sum_{i=0}^{N-1} |I(j,i) - I'(j,i)|^2, \tag{6}$$

where M and N are the image dimension and j and i indicate each pixel position.

We also recall the Parseval's equality for the energy conservation in the signal domain and the transform domain.

Definition 2. In the *Parseval's Equality*, the energy is conserved between an input signal and the transform domain coefficient in the case of an orthonormal filter bank wavelet base.[16] Assuming the input signal $x[n]$ with the length of $n \in Z$ and the corresponding transformed domain coefficients of $y[k]$ where $k \in Z$, according to energy conservation theorem,

$$\|x\|^2 = \|y\|^2. \tag{7}$$

On the other hand non-orthonormal wavelets such as biorthogonal wavelets do not hold conservation of energy. But for a stable expansion, the transform domain coefficients have to satisfy the Eq. (8).[16]

$$A \sum_k |y[k]|^2 \leq \|x\|^2 \leq B \sum_k |y[k]|^2, \tag{8}$$

where A and B are the orthonormality correction factor.

Based on the discussed propositions and the definitions we shall build the extended model and make the new propositions.

As suggested in Eq. (8), for a non-orthonormal wavelet base an orthonormality correction factor is required and we shall call this as a weighting factor W which is defined as follows:

$$W = \frac{\|x\|^2}{\sum_k |y[k]|^2}, \tag{9}$$

where x and y is the input signal and the transform domain coefficients, respectively.

We consider the polyphase matrix representation of the discrete wavelet transform (DWT)[17] and its reconstruction. The inverse DWT can be defined by a synthesis filter bank using the polyphase matrix $M'(z) = \begin{pmatrix} h'_e(z) & h'_o(z) \\ g'_e(z) & g'_o(z) \end{pmatrix}$ where $h'(z)$ represents the low pass filter coefficients and $g'(z)$ is the high pass filter coefficients and the subscripts e and o denote even and odd indexed terms, respectively. The transform domain coefficient y can be re-mapped into input signal x as bellow:

$$\begin{pmatrix} x_e(z) \\ x_o(z) \end{pmatrix} = \begin{pmatrix} h'_e(z) & h'_o(z) \\ g'_e(z) & g'_o(z) \end{pmatrix} \begin{pmatrix} y_e(z) \\ y_o(z) \end{pmatrix}. \tag{10}$$

Considering Δy is the noise introduced in wavelet domain and Δx is the modified signal after the inverse transform, using the *Linearity* property of the Z transform of the filter coefficients and signals in the polyphase matrix, it is proved in our previous work[13] that

$$\begin{pmatrix} \Delta x_e(z) \\ \Delta x_o(z) \end{pmatrix} = \begin{pmatrix} h'_e(z) & h'_o(z) \\ g'_e(z) & g'_o(z) \end{pmatrix} \begin{pmatrix} \Delta y_e(z) \\ \Delta y_o(z) \end{pmatrix}. \tag{11}$$

In a polyphase decomposition we use different low pass and high pass filter banks. Therefore at each of the different transform points, we receive different weighting factors W^g and W^h, corresponding to high or low pass filters, respectively. Now the *Proposition 2* can be extended as follows, accommodating the weighting factors for non-orthonormal transforms:

$$\begin{aligned} \sum (|\Delta x_e|^2 + |\Delta x_o|^2) &= W^g \sum (|\Delta y_e|^2 + |\Delta y_o|^2) + W^h \sum (|\Delta y_e|^2 + |\Delta y_o|^2), \\ \sum_n |\Delta x[n]|^2 &= W^g \sum (|\Delta y_e|^2 + |\Delta y_o|^2) + W^h \sum (|\Delta y_e|^2 + |\Delta y_o|^2). \end{aligned} \tag{12}$$

Now using the generalised framework, and the extension of the *Proposition 1*, the Eq. (12) can be applied to build the relationship between the modification energy in the coefficient domain to embed the watermark and the distortion performance metrics for orthonormal as well as non-orthonormal wavelet bases.

Proposition 3. *In a wavelet based watermarking scheme, the mean square error (MSE) of the watermarked image is directly proportional to the weighted sum of the energy of the modification values of the selected wavelet coefficients.*

$$P_p \propto \sum W^{\Theta\Upsilon} |\Delta_{m,n}|)|^2, \tag{13}$$

where W is the weighting parameter at each subband and Θ represents the subband no. at Υ decomposition level.

The modification value itself is a function of the wavelet coefficients and therefore, we propose an example case of direct modification, based on the general framework.

Example Case. *For the direct modification embedding method the modification is a function of the selected coefficient to be watermarked and the relationship between MSE (P_p) and the selected coefficient ($C_{m,n}$) is expressed as:*

$$P_p \propto \sum W^{\Theta\Upsilon} |f(C_{m,n})|^2, \tag{14}$$

where W is the weighting parameter at each subband and Θ represents the subband no at Υ decomposition level.

Proof. The watermark embedding is generally performed by modifying the wavelet coefficients in any wavelet based algorithms. Due the modification, an error is introduced in transform domain which is similar to any noise in the transform domain. Therefore, the sum of the energy of the modification value due to watermark embedding in the wavelet domain is equal to the sum of the noise energy in the transform domain. From Eq. (1) and Eq. (3), the energy sum of the modification value $\Delta_{m,n}$ can be defined as:

$$\sum_{m,n} |\Delta_{m,n}|^2 = \sum_{k} |\Delta y[k]|^2. \tag{15}$$

Similarly, the pixel domain distortion performance metrics which is represented by MSE is considered as the noise error created in the signal due to the noise in wavelet domain. Therefore, the sum of the noise energy in the input signal is equal to the sum of the noise error energy P_p in the pixel domain:

$$P_p.(MN) = \sum_{n} |\Delta x[n]|^2, \tag{16}$$

where M and N are the image dimensions. Now the relationship between the distortion performance metric MSE of the watermarked image and the coefficient modification value which is normally a function of the selected wavelet coefficients can be decided using the extended *Proposition 1.*

Thus from with the help of Eq. (12), combining Eq. (15) and Eq. (16), we can write:

$$P_p.(MN) \quad = \textstyle\sum_{m,n} W^g |\Delta_{m,n}|^2 + \sum_{m,n} W^h |\Delta_{m,n}|^2, \tag{17}$$

where M and N are the image dimensions. Hence for any watermarked image, the average noise power P_p is proportional to the sum of the energy of the modification values of the selected wavelet coefficients:

$$P_p \quad \propto \textstyle\sum_{m,n} W^g |\Delta_{m,n}|^2 + \sum_{m,n} W^h |\Delta_{m,n}|^2. \tag{18}$$

Now in the case of 2-D wavelet decompositions, the wavelet kernel transfer function, for each subband at each decomposition level are different and so that the weighting factors are. Hence the Δ in Eq. (18) are associated with a corresponding weighting parameter for each subband at each decomposition level. We define the weighting parameter as $W^{\Theta\Upsilon}$ at each subband and Θ represents the subband no. at Υ decomposition level.

With the help of the common framework a relationship is established between the error energy of the watermarked image and the selected wavelet coefficient energy of the host image. For example, a direct modification based algorithm, the mean square error P_p is directly proportional to the weighted sum of the energy of the modification value Δ which is a function of wavelet coefficient value as stated below:

$$P_p \propto \sum W^{\Theta\Upsilon} |f(C_{m,n})|^2 \ . \tag{19}$$

where W is the weighting parameter at each subband and Θ represents the subband no. at Υ decomposition level.

For an orthonormal wavelet kernels the value of the weighting parameters are equal to unity whereas for a non-orthonormal wavelet kernel, different weighting parameter values are suggested for different subbands at each decomposition level.

■

4. EXPERIMENTAL SIMULATIONS

Experimental simulations have been carried out to verify the propositions made in the previous section. There are two different parts of the experiment conducted: calculation of the weighting parameters and simulation of the propositions.

4.1 Calculation of the weighting parameters

The weighting parameters are calculated for each subband at each decomposition level for various wavelet kernels. We have done a three level decomposition and calculated the weighting parameter value for each of the ten subbands. A set of different non-orthonormal wavelet kernels including 5/3, 9/7, spline 9/3, spline 16/4, 9/11-A and 9/11-B[18] are chosen for the experiments. We have considered the energy ratio (refer Eq. (20)) for each subband one at a time while keeping other subband values to zero.

$$W^{\Theta\Upsilon} = \frac{\|x\|^2}{\sum |y^{\Theta\Upsilon}|^2}, \tag{20}$$

where $W^{\Theta\Upsilon}$ is the weighting parameter at Θ subband at Υ decomposition level, $y^{\Theta\Upsilon}$ is the coefficient value at Θ subband at Υ decomposition level and x is the output pixel values after the inverse wavelet transform. The weighting parameters are calculated for the experimental image set and generalised by averaging them. It is observed that these parameters are image independent. The corresponding weighting parameters for different subbands at each decomposition levels are calculated and shown Tab. 2 along with the error. The errors presented here display accuracy up to the 95% confidence interval.

Table 2. Weighting parameter values of each subband at each decomposition level for various non-orthonormal wavelets

	5/3	9/7	9/3	16/4	9/11A	9/11B
LL3	0.97±0.01	1.00±0.00	0.97±0.01	0.94±0.01	1.01±0.00	0.86±0.03
LH3	0.55±0.02	1.11±0.01	0.53±0.02	0.25±0.02	1.91±0.07	0.13±0.01
HL3	0.56±0.02	1.14±0.01	0.52±0.02	0.24±0.02	1.99±0.07	0.12±0.01
HH3	0.52±0.01	1.09±0.02	0.46±0.01	0.18±0.01	2.15±0.01	0.11±0.01
LH2	0.70±0.03	1.04±0.02	0.66±0.03	0.38±0.03	1.46±0.05	0.27±0.03
HL2	0.66±0.02	1.04±0.01	0.65±0.02	0.34±0.02	1.49±0.04	0.25±0.02
HH2	0.79±0.02	0.97±0.02	0.74±0.02	0.40±0.02	1.23±0.01	0.40±0.02
LH1	1.29±0.04	1.10±0.01	1.27±0.04	1.43±0.08	0.91±0.02	1.53±0.11
HL1	1.30±0.03	1.10±0.01	1.27±0.03	1.45±0.07	0.92±0.02	1.49±0.09
HH1	2.41±0.07	1.18±0.02	2.34±0.07	4.28±0.24	0.59±0.01	6.46±0.41

4.2 Simulations of the propositions

For the simulation purpose we have chosen one example case[2] of direct modification from the generalised framework. Two different sets of results are obtained and displayed to verify the effects of different input parameters which are responsible for embedding distortion performance. These two sets of experimental arrangements and resulting plots are discussed separately as follows:

- In the experiment *Set 1*, the un-weighted and the weighted sum of energy of the selected wavelet coefficients to be modified and MSE of the watermarked image have been calculated using the same α and the same binary watermark logo. A set of combinations of the subbands have been used to embed the watermark. For example, after three level of wavelet decompositions, ten subbands are created such as LL3, HL3, LH3 and HH3 at 3rd decomposition level, HL2, LH2 and HH2 at 2nd decomposition level and HL1, LH1 and HH1 at 1st decomposition level. Now six combinations have been chosen for the experiments: AF3 (LL3, HL3, LH3 and HH3), AF2 (LL3, HL3, LH3, HH3, HL2, LH2 and HH2), AF1 (LL3, HL3, LH3, HH3, HL2, LH2, HH2, HL1, LH1 and HH1), HF3 (HL3,LH3 and HH3), HF2 (HL2, LH2 and HH2) and HF1

Table 3. Correlation coefficient values between sum of energy and the MSE for different wavelet kernel in various subband combinations

	5/3	9/7	9/3	16/4	9/11A	9/11B
AF3	0.99	0.99	0.99	0.99	0.99	0.98
AF2	0.99	0.99	0.99	0.99	0.99	0.98
AF1	0.99	0.99	0.99	0.99	0.99	0.98
HF3	0.98	0.99	0.98	0.95	0.98	0.95
HF2	0.99	0.99	0.99	0.97	0.99	0.96
HF1	0.99	0.99	0.99	0.97	0.99	0.97

(HL1, LH1 and HH1). We have used various non-orthonormal wavelet kernels including 5/3, 9/7, spline 9/3, spline 16/4, 9/11-A and 9/11-B and observed the results for each selected subband combination. The correlation plots of MSE vs. un-weighted energy sum and MSE vs. weighted energy sum is displayed in Fig. 1 and Fig. 2. In each of the figures *Row 1* represents MSE vs. the un-weighted energy sum and *Row 2* represents corresponding plots after applying the weighting parameters. The correlation coefficients of the weighted energy sum are also calculated and presented in Tab. 3.

In another representation, a set of graphs are plotted in Fig. 3 and Fig. 4. These plots present the average values of the MSE, un-weighted and the weighted sum of energy for the test image set. In each of the figures *Column 1* presents average MSE, *Column 2* presents un-weighted average energy sum and *Column 3* represents weighted average energy sum. The error bars denote the accuracy up to the 95% confidence interval. In these graphs the trends have been compared for MSE vs un-weighted energy sum and the trend after weighting correction.

- In the experiment *Set 2*, the performance for different subband combinations are plotted for each wavelet kernel in a similar fashion as mentioned in experiment *Set 1* in order to observe the trend. The results are shown in Fig. 5 and Fig. 6 and in each of the figures *Column 1* presents average MSE, *Column 2* presents un-weighted average energy sum and *Column 3* represents weighted average energy sum. As earlier, a 95% confidence interval is considered which is denoted by the error bars.

From the results it is observed that the proportionality relation does not exist or poorly presents in case of a un-weighted energy sum. But with the introduction of the weighting parameters, a strong proportionality relation is observed for each individual subband combination or wavelet kernel, as suggested in the proposition as shown in Fig. 1 and Fig. 2. On the other hand, in the pattern graphs in Fig. 3, Fig. 4, Fig. 5 and Fig. 6, the MSE and the un-weighted energy sum graph patterns does not show similarity whereas a pattern similarity is regained after applying the weighting parameters. Also a strong correlation of more than 0.95 is observed between MSE of the watermarked image and the weighted energy sum of the selected wavelet coefficients to be modified.

An extensive simulation is performed using 25 different images from Kodak data base and the results strongly support the proposed model for a wide range of input images and various non-orthonormal wavelet kernels.

5. CONCLUSIONS

A universal embedding distortion performance model is presented here for wavelet based watermarking schemes. We have extended our previous model which considers only orthonormal wavelet kernels, to non-orthonormal wavelet kernels such as biorthogonal and non-linear wavelets. The current model suggests that the MSE of the watermarked image is directly proportional to the weighted sum of energy of the modification values of the selected wavelet coefficients and this proposition is valid for orthonormal as well as non-orthonormal wavelet kernels. In the case of the non-orthonormal wavelet bases a weighting parameter is introduced and it is computed experimentally for different non-orthonormal wavelet bases. This universal model is verified by experimental simulations with a wide range of wavelet kernels.

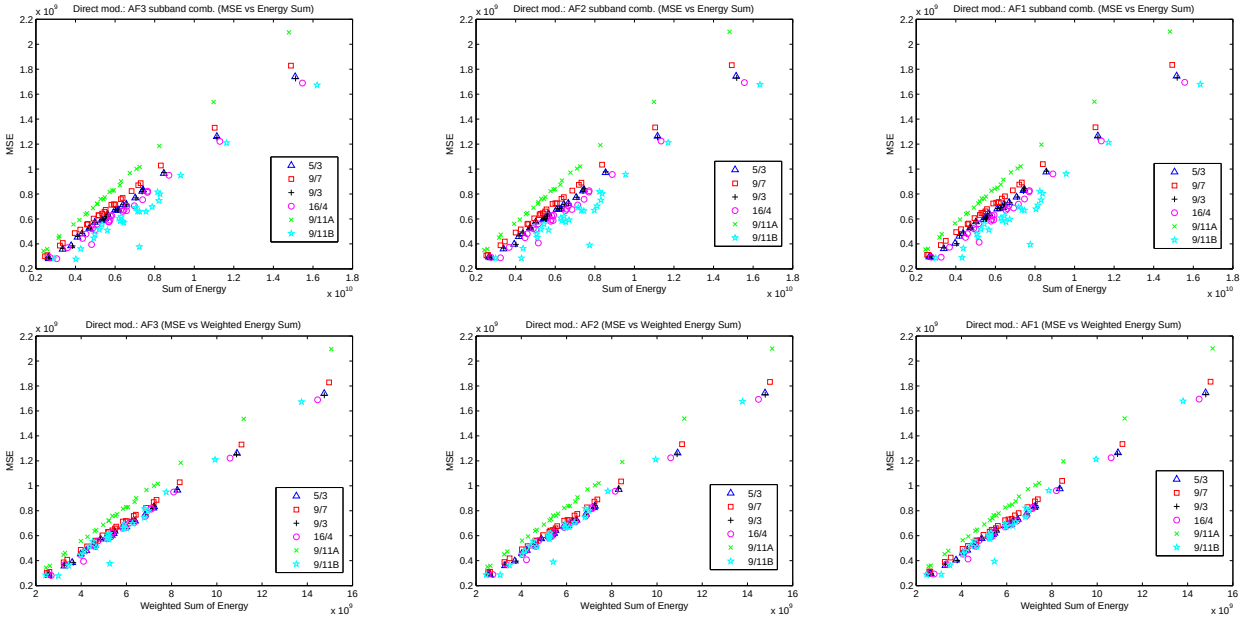

Figure 1. Correlation plots: MSE vs. sum of energy for different subband combinations. Wavelets used: 1. 5/3 2.9/7 3.9/3 4.16/4 5.9/11A 6.9/11B. *Row 1*: Without weighting parameter, *Row 2*: with weighting parameter.

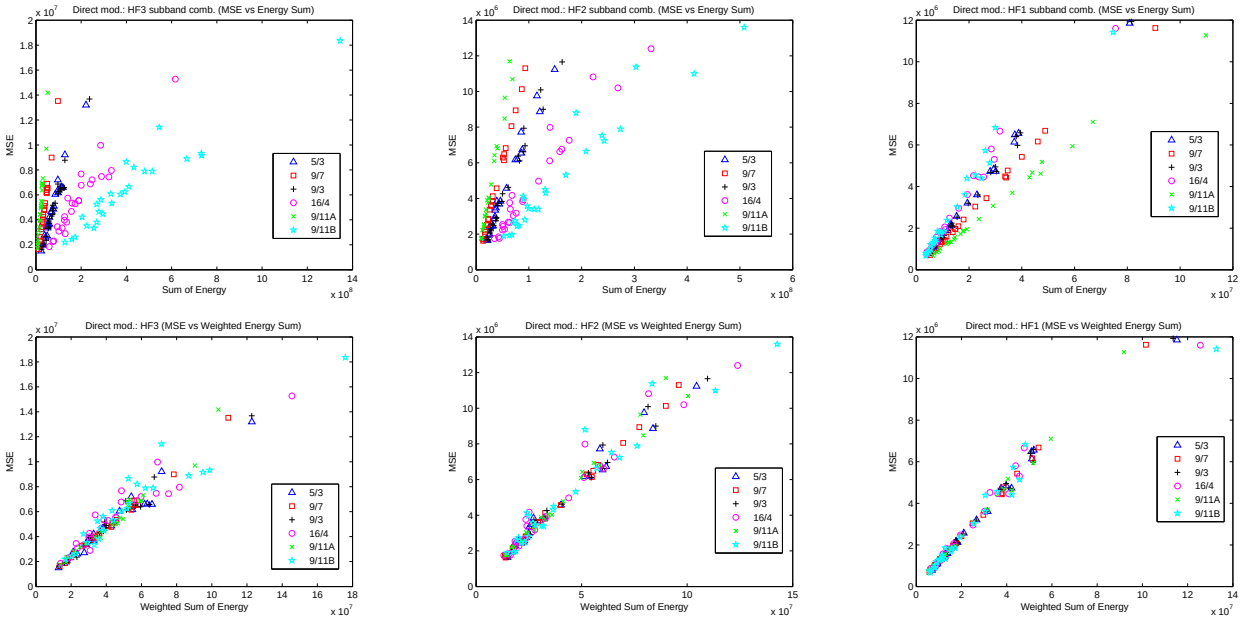

Figure 2. Correlation plots: MSE vs. sum of energy for different subband combinations. Wavelets used: 1. 5/3 2.9/7 3.9/3 4.16/4 5.9/11A 6.9/11B. *Row 1*: Without weighting parameter, *Row 2*: with weighting parameter.

Acknowledgments

This work is funded by BP-EPSRC Dorothy Hodgkin postgraduate award.

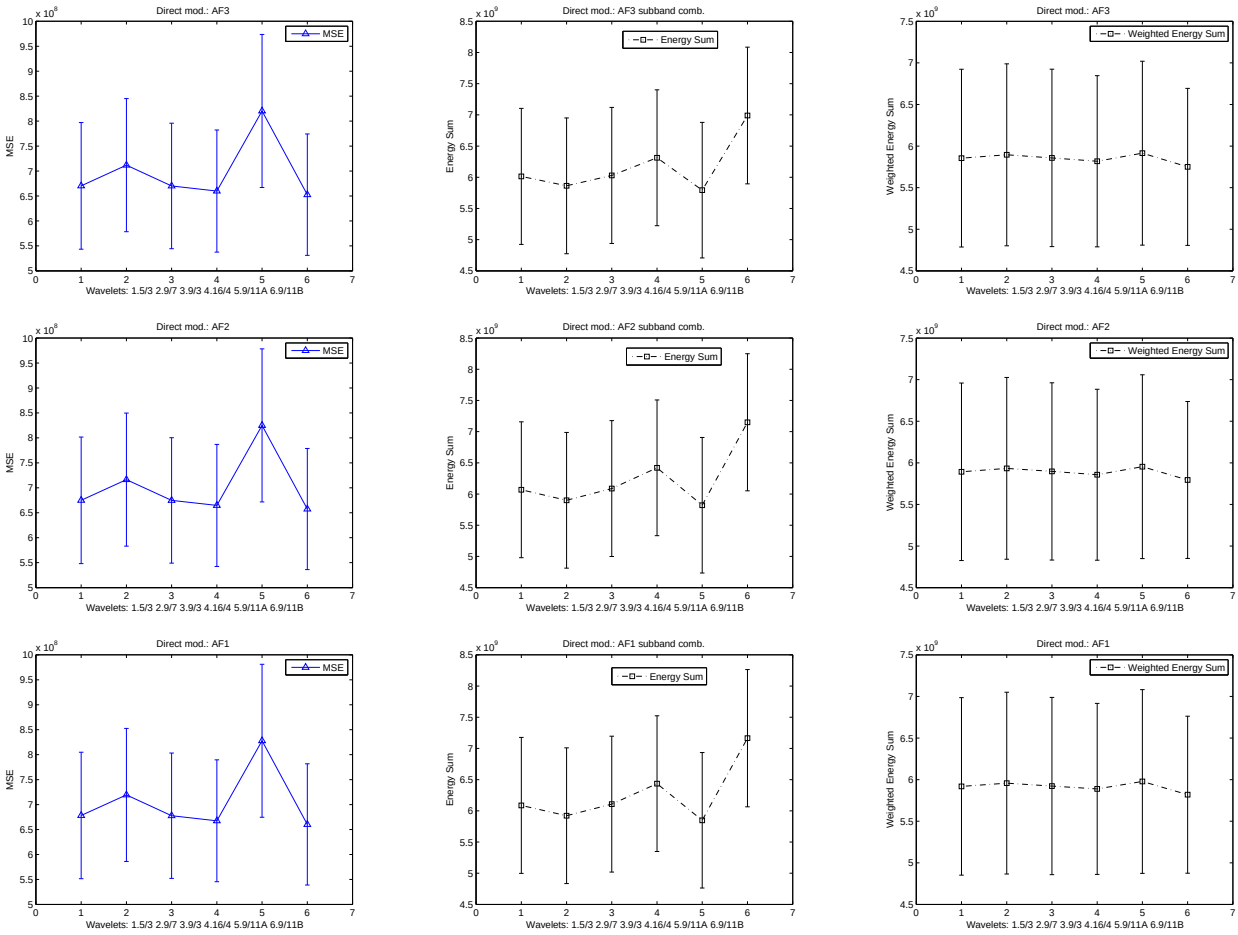

Figure 3. Similarity pattern graph among MSE, un-weighted energy sum and weighted energy sum for different subband combinations. Wavelets used: 1. 5/3 2.9/7 3.9/3 4.16/4 5.9/11A 6.9/11B. *Column 1*: Average MSE, *Column 2*: Average un-weighted energy sum, *Column 3*: Average weighted energy sum.

REFERENCES

[1] Xia, X., Boncelet, C. G., and Arce, G. R., "Wavelet transform based watermark for digital images," *Optic Express* **3**, 497–511 (Dec. 1998).

[2] Kim, J. R. and Moon, Y. S., "A robust wavelet-based digital watermarking using level-adaptive thresholding," in [*Proc. IEEE ICIP*], **2**, 226–230 (1999).

[3] Huo, F. and Gao, X., "A wavelet based image watermarking scheme," in [*Proc. IEEE ICIP*], 2573–2576 (Oct. 2006).

[4] Kundur, D. and Hatzinakos, D., "Digital watermarking using multiresolution wavelet decomposition," in [*Proc. IEEE ICASSP*], **5**, 2969–2972 (May 1998).

[5] Wang, H.-J., Su, P.-C., and Kuo, C.-C. J., "Wavelet-based digital image watermarking," *Optics Express* **3**, 491–497 (Dec. 1998).

[6] Xie, L. and Arce, G. R., "Joint wavelet compression and authentication watermarking," in [*Proc. IEEE ICIP*], **2**, 427–431 (1998).

[7] Barni, M., Bartolini, F., and Piva, A., "Improved wavelet-based watermarking through pixel-wise masking," *IEEE Trans. Image Processing* **10**, 783–791 (May 2001).

[8] Jin, C. and Peng, J., "A robust wavelet-based blind digital watermarking algorithm," *Information Technology Journal* **5**(2), 358–363 (2006).

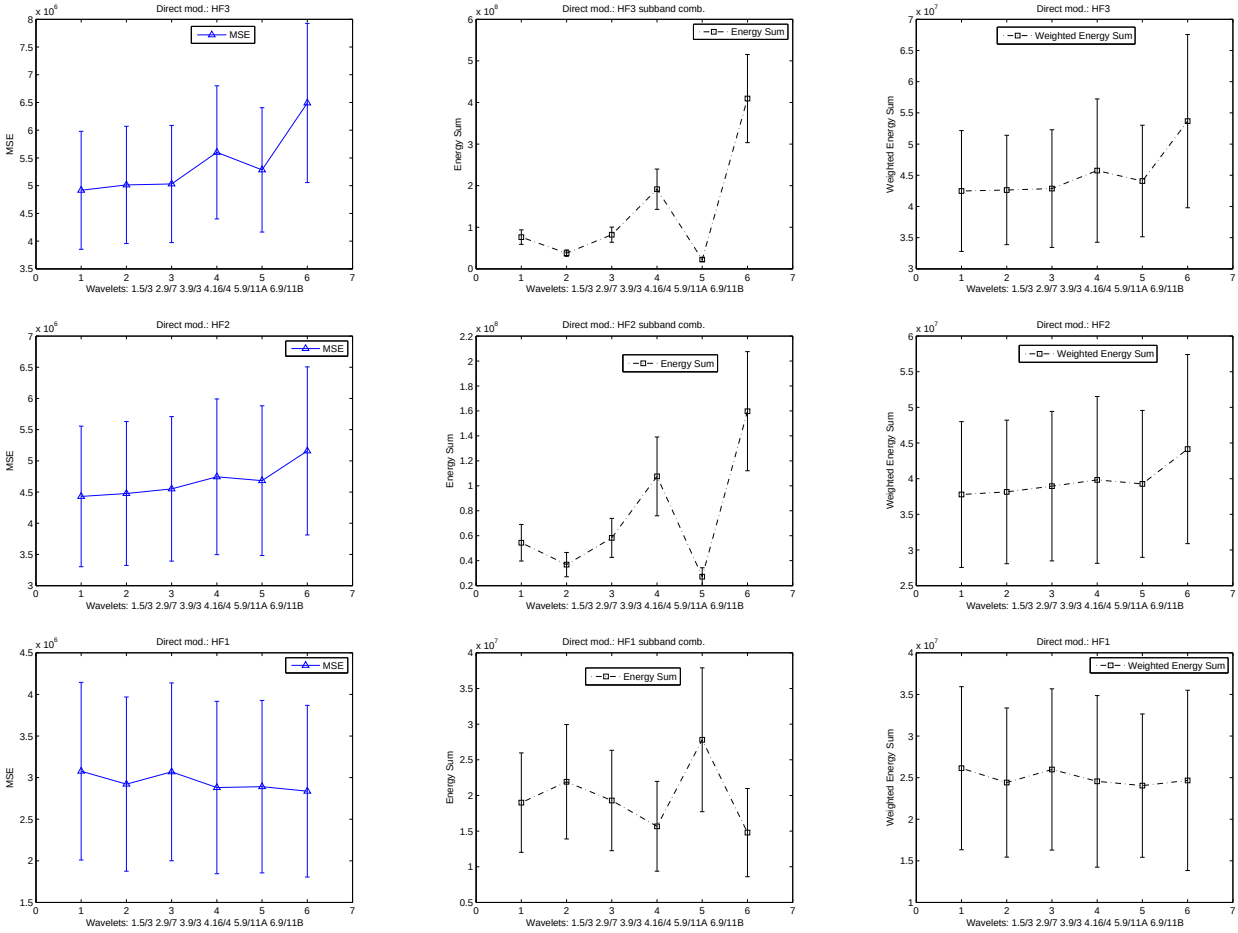

Figure 4. Similarity pattern graph among MSE, un-weighted energy sum and weighted energy sum for different subband combinations. Wavelets used: 1. 5/3 2.9/7 3.9/3 4.16/4 5.9/11A 6.9/11B. *Column 1*: Average MSE, *Column 2*: Average un-weighted energy sum, *Column 3*: Average weighted energy sum.

[9] Gong, Q. and Shen, H., "Toward blind logo watermarking in JPEG-compressed images," in [*Proc. Int'l conf. on parallel and distributed computing, applications and technologies (PDCAT 2005)*], 1058–1062 (Dec. 2005).

[10] Feng, X. C. and Yang, Y., "A new watermarking method based on DWT," *Lect. Notes in Comp. Sc.* **3802**, 1122–1126 (2005).

[11] Kundur, D. and Hatzinakos, D., "Toward robust logo watermarking using multiresolution image fusion principles," *IEEE Trans. Multimedia* **6**, 185–198 (Feb. 2004).

[12] Ejima, M. and Miyazaki, A., "On the evaluation of performance of digital watermarking in the frequency domain," in [*Proc. IEEE ICIP*], **2**, 546–549 (Oct. 2001).

[13] Bhowmik, D. and Abhayaratne, C., "A generalised model for distortion performance analysis of wavelet based watermarking," in [*Proc. 7th Int'l Workshop on Digital Watermarking (IWDW '08), Lect. Notes in Comp. Sc.*], (Nov. 2008).

[14] Bhowmik, D. and Abhayaratne, C., "Evaluation of watermark robustness to JPEG2000 based content adaptation attacks," in [*Proc. IET Int'l Conf. on Visual Info. Eng. (VIE '08)*], 789–794 (Jul.-Aug. 2008).

[15] Zhang, Z. and Mo, Y. L., "Embedding strategy of image watermarking in wavelet transform domain," in [*Proc. Image Compression and Encryption Technologies*], **4551**(1), 127–131, SPIE (2001).

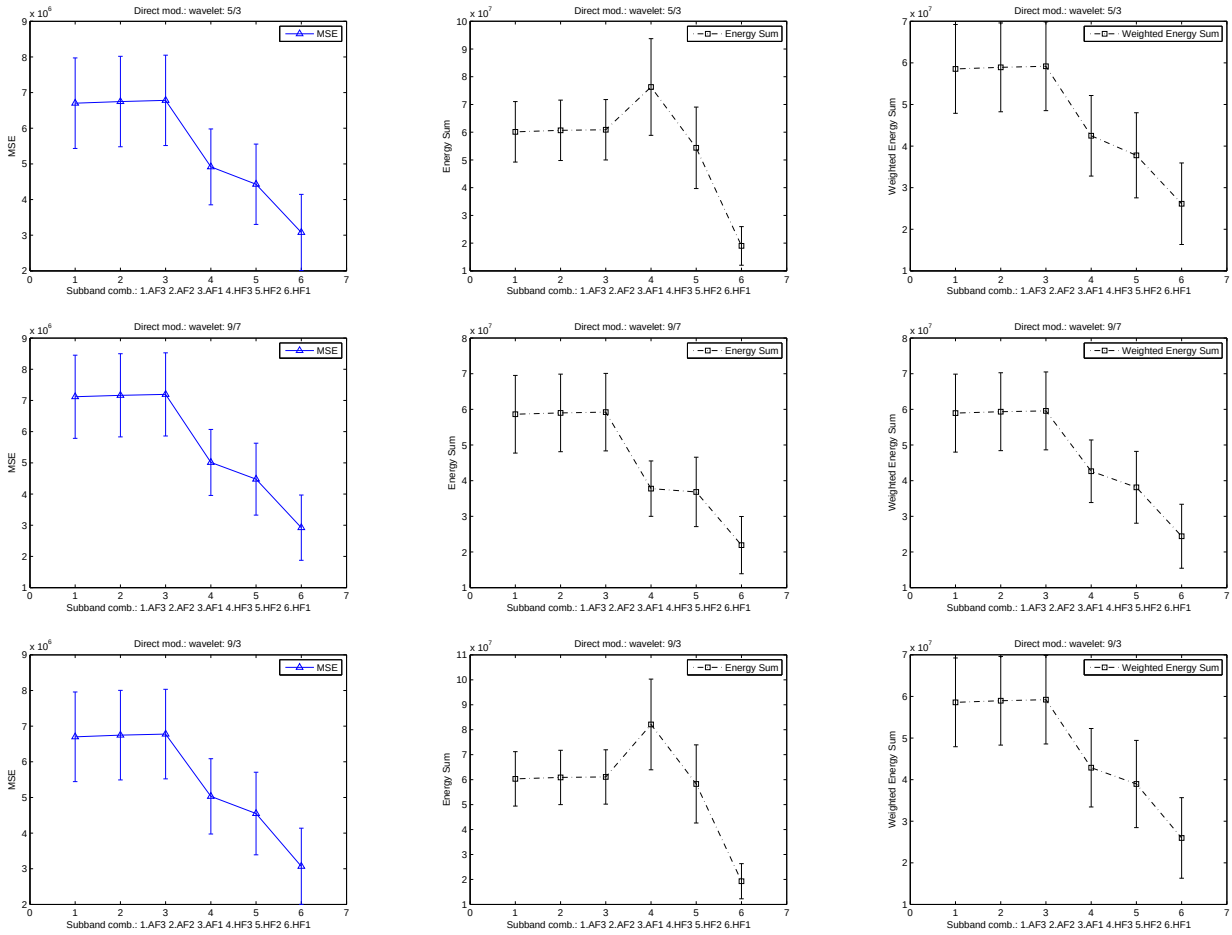

Figure 5. Similarity pattern graph among MSE, un-weighted energy sum and weighted energy sum for different wavelet kernels. Subband combinations used: 1. AF3 2.AF2 3.AF3 4.HF3 5.HF2 6.HF1. *Column 1*: Average MSE, *Column 2*: Average un-weighted energy sum, *Column 3*: Average weighted energy sum. AF3, AF2 and AF1 values are scaled to fit in the same graph.

[16] Vetterli, M. and Kovačevic, J., [*Wavelets and subband coding*], Prentice-Hall, Inc., Upper Saddle River, NJ, USA (1995).

[17] Daubechies, I. and Sweldens, W., "Factoring wavelet transforms into lifting steps," *J. Fourier Anal. Appl.* **4**(3), 245–267 (1998).

[18] Mallat, S., [*A Wavelet Tour of Signal Processing*], Academic Press (1997).

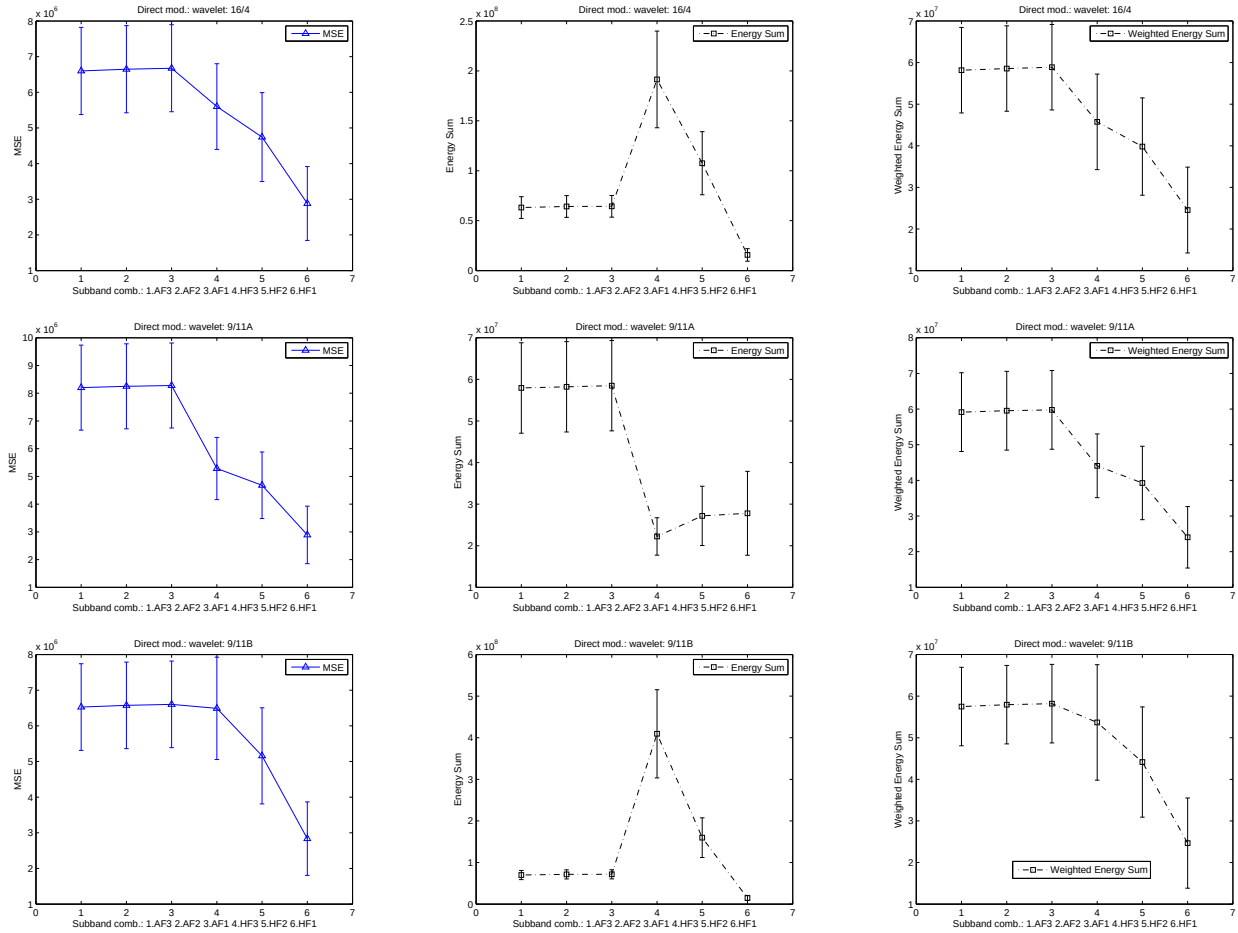

Figure 6. Similarity pattern graph among MSE, un-weighted energy sum and weighted energy sum for different wavelet kernels. Subband combinations used: 1. AF3 2.AF2 3.AF3 4.HF3 5.HF2 6.HF1. *Column 1*: Average MSE, *Column 2*: Average un-weighted energy sum, *Column 3*: Average weighted energy sum. AF3, AF2 and AF1 values are scaled to fit in the same graph.